HIGHLIGHTED STUDENT RESEARCH



Visible and near-infrared hyperspectral indices explain more variation in lower-crown leaf nitrogen concentrations in autumn than in summer

Kathryn I. Wheeler^{1,2} · Delphis F. Levia^{1,3} · Rodrigo Vargas^{1,3}

Received: 25 January 2019 / Accepted: 5 November 2019 / Published online: 27 November 2019 © Springer-Verlag GmbH Germany, part of Springer Nature 2019

Abstract

Autumn canopy phenological transitions are increasing in length as a consequence of climate change. Here, we assess how well hyperspectral indices in the visible and near-infrared (NIR) wavelengths predict nitrogen (N) concentrations in lower-canopy leaves in the autumn phenological transition as they are generally understudied in leaf trait research. Using a Bayesian framework, we tested how well published indices are able to predict N concentrations in *Fagus grandifolia* Ehrh., *Liriodendron tulipifera* L., and *Betula lenta* L. from mid-summer through senescence, and how related the indices are to autumn phenological change. No indices were able to determine a trend in differences in N in mid-summer leaves. Indices that included wavelengths in the green and NIR ranges were the first indices able to detect a trend and had among the highest correlations with N concentration in both the last green collection and the senescing collection. Models were unique when indices were fit to data from different phenophases. Indices that focused on only the red edge (i.e., the sharp increase in reflectance between the red and NIR wavelengths) had the strongest explanatory power across the autumn phenological transition, but had less explanatory power for individual collections. These indices, as well as those that have been correlated with chlorophyll (CCI) and carotenoids (PRI), were the strongest descriptors of autumn progression. This study provides insights on challenges and capabilities to monitor a leaf's N concentration throughout and across canopy senescence.

 $\textbf{Keywords} \ \ Phenology \cdot Leaf \ traits \cdot Resorption \cdot Autumn \cdot Hyperspectral$

Communicated by David R. Bowling.

Autumn has been extended in Northern Hemisphere forests due to progressive climate change. Most past studies that aim to quantify canopy-scale changes during the autumn, using hyperspectral remotely sensed observations, have relied on trait spectra relationships for sunlit green leaves. We discovered that certain hyperspectral indices are effective at predicting leaf nitrogen concentrations and other traits in the lower canopy throughout the fall, improving our ability to remotely monitor changes in canopy physiology.

Electronic supplementary material The online version of this article (https://doi.org/10.1007/s00442-019-04554-2) contains supplementary material, which is available to authorized users.

Kathryn I. Wheeler kiwheel@bu.edu

Extended author information available on the last page of the article

Introduction

One of the most visible impacts of global environmental change is the effect of rising air temperatures on the lengthening of the growing season in temperate deciduous forests (Parmesan and Yohe 2003). While the timing of phenological transitions in both spring and autumn is changing, less than 50% as many climate change studies are set in autumn than in spring (Gallinat et al. 2015). Phenological spring transitions occur at a much shorter time scale than autumn ones and, thus, the autumn transition is harder to model and predict (Richardson et al. 2012). Part of the confusion around predicting and quantifying the length and timing of autumn transitions is due to differences in definitions of senescence (Gill et al. 2015) and in methods for measuring the timing of this transition, which can result in different conclusions of how it is changing (Keenan et al. 2014). Regardless, numerous studies have found that the autumn phenological transition is often being lengthened or delayed in temperate deciduous forests (Linderholm 2006; Gill et al.



2015). Autumn is physiologically important because it is when trees prepare for winter dormancy, with preparation starting well before visual changes are apparent in leaf color (Estiarte and Peñuelas 2015). These less evident responses include a decrease in tree photosynthesis and respiration (McKown et al. 2013) later in summer months before leaf abscission. Studies of leaf traits and remote sensing of traits predominantly focus on peak-green leaves (Yang et al. 2016), however many traits and trait relationships have large phenological variation even within the green canopy (McKown et al. 2013). With the changes to autumn phenological transitions, understanding how traits and trait relationships change throughout autumn is becoming more important in understanding net annual changes. Specifically, understanding and measuring those leaf traits that are known to change in the autumn, such as leaf nitrogen (N) concentrations, is increasingly important.

N can be a growth-limiting nutrient as it is in short supply in many deciduous forest ecosystems and is essential to photosynthesis (LeBauer and Treseder 2008). N is found in a variety of proteins in the cell with 50-60% of the N in many leaves contained in the chloroplasts (Mostowska 2005), half of which is in the enzyme Rubisco and small amounts in chlorophyll. Between 10 and 15% of the N is typically in nucleic acids (Chapin and Kedrowski 1983) and around 9% is in proteins attached to cell walls (Onoda et al. 2004). Especially if N is limited, a tree often does not invest the same amount of N in each of its leaves and instead focuses on investing N in leaves with greater photosynthetic potential, such as sunlit, upper-crown leaves (Hikosaka 2016). This often results in a greater percentage of N in upper-crown leaves being allocated to the photosynthetic apparatus than that allocated in shaded, lower-crown leaves. In autumn, deciduous trees will break down organelles in their leaves and reabsorb the N for storage in the woody tissues to use in spring growth, which initially is almost exclusively due to stored N (Neilsen et al. 1997). N that is not resorbed before leaf abscission enters the rest of the ecosystem and may not be available to the tree for initial spring growth. Along with lignin concentrations, the N concentrations of leaf litter affect the decomposition rate (Berg and McClaugherty 2003), accumulation of soil organic matter (Berg and Meentemeyer 2002), and N mineralization rate (Inagaki et al. 2004). Extending senescence is associated with increasing N resorption (Inagaki et al. 2010), but this increases the risk that the leaves will be detached prematurely before N resorption has completed.

Leaves do not only fall in the autumn after senescence and resorption have completed. Changes in the levels and gradients of the hormones auxin and ethylene in leaves (Morgan 1984; Taiz and Zeiger 2006) make it easier for not only the tree to shed leaves that are not worth the investment, but also for autumn storms to prematurely detach leaves.

Hurricanes and other storms can also result in greenfall, even before physiological changes in the leaves have started to occur (Vargas 2012). Additionally, as many of the phenological changes are being delayed with climate change, the risk of early frosts causing premature leaf abscission also increases, which has been observed in the spring (Richardson et al. 2018). Thus, increasing the risk of premature leaf abscission makes it more important to be able to measure N concentrations in leaves throughout the autumn phenological transition.

Hyperspectral remote sensing of N in leaves and canopies is an ideal way to monitor N concentrations in a nondestructive manner because macromolecules in leaves reflect and absorb light at specific wavelengths. Leaf reflectance spectra give information about pigment concentrations in the visible region (400-700 nm), leaf structure in the nearinfrared region (700-1300 nm, NIR), and water and proteins in the shortwave infrared region (1300–2500 nm, SWIR) (Homolová et al. 2013). Because N is a primary component in some compounds (e.g., chlorophyll, proteins), indices and other hyperspectral evaluation methods that include wavelengths in all three ranges typically are better at predicting N concentrations than indices that only include one or two of the wavelength ranges (Serbin et al. 2014; Yang et al. 2016). Due to the expense of SWIR instruments, many studies have focused on the ability of hyperspectral indices in the visible and NIR wavelengths at predicting N concentrations with the justification that chlorophyll concentrations have been found to often be correlated with N concentrations in sunlit green leaves (Sage et al. 1987; Homolová et al. 2013; Noda et al. 2015). Many of these indices rely on ratios between wavelengths in the red and NIR region, which is commonly referred to as the "red edge". Most studies have focused on sunlit leaves, as canopy reflectance of top-of-canopy leaves can be measured by airborne and satellite platforms.

The majority of leaves, however, exist under shaded conditions (Keenan and Niinemets 2016) and, thus, N may not be as closely tied to chlorophyll in these green leaves. Ratios between chlorophyll and N concentrations have been found to vary greatly throughout the year (Croft et al. 2017). Yang et al. (2016) investigated how leaf spectra-trait relationships vary between seasons and found that the relationships between spectra and N concentrations vary greatly between spring, summer, and autumn. They, however, primarily focused on sunlit leaves and included spectra through the SWIR. They defined autumn as starting when leaf chlorophyll starts to decrease and did not look at variation within this autumn period. With climate change altering the duration of this autumn phenological transition, it is becoming more important to understand variation with leaf spectra-trait relationships within autumn. Thus, there is a pressing need to identify hyperspectral indices in the visible and NIR that are able to explain variation in leaf N



concentrations. This effort will allow the determination of the relationships between different hyperspectral indices and changes in N concentrations of lower-crown leaves throughout the course of the autumn phenological change.

For this study, we selected a variety of published hyperspectral indices in the visible and NIR ranges that were found to be correlated with pigment concentrations or that have a strong phenological signal. We collected lower-crown leaves from Fagus grandifolia Ehrh. (American beech), Liriodendron tulipifera L. (yellow poplar), and Betula lenta L. (sweet birch) five times from mid-summer through senescence and fit regression models to investigate which indices are the strongest at predicting leaf N across autumn and how explanatory power of the indices and their relationships with N concentrations changes between collections. We also tracked how the indices changed throughout the autumn transition in situ on trees to determine which indices have the strongest phenological signals and investigate if the indices with the highest N predictive power are the same as the ones with the most consistent phenological change (i.e., have the strongest trend of change in autumn). Our two primary hypotheses were (1) the indices will not be correlated with N concentrations in the mid-summer green leaves due to likely weak correlations between pigments and N in lower-crown leaves, but will overall increase in explanatory power as the autumn transition progresses with N resorption resulting in stronger correlations between N concentrations and chlorophyll in the lower-crown leaves, and (2) the indices that have been shown to be strong descriptors of autumnal change will not be the strongest predictors of leaf N across autumn if they involve changes in pigments other than chlorophyll. We aimed to identify indices that are able to improve our knowledge of a leaf's N concentration at different points during the autumn and test the sensitivity of the relationships across phenophases.

Methods

Site description

We measured trees in the Fair Hill Natural Resources Management Area in Elkton, Maryland. Fair Hill is in the Chesapeake Bay Watershed and is situated just northwest of the Fall Line between the Piedmont and the Atlantic Coastal Plain. The local climate is characterized by relatively constant precipitation throughout the year. From 1981–2010, the mean annual precipitation was 1205 mm, the 30-year mean maximum air temperature was 19.1 °C, and the 30-year mean minimum temperature was 6.8 °C (NCDC 2014). The forest type is mixed deciduous with dominant tree species of *F. grandifolia*, *L. tulipifera*, and *B. lenta*. Soils are predominantly silt loams and have igneous, metamorphic,

phyllite and schist parent material (USDA NRCS USDA NRCS 2003). Soils were previously found to have total N, ammonium-bound N, and nitrate-bound N concentrations of 0.129%, 5.13 mg/kg, and 1.21 mg/kg, respectively (Wheeler et al. 2017).

Field data collection

Tree and leaf selection

Between August and mid-November of 2016, we collected in situ temporal hyperspectral data from five *F. grandifolia*, five *B. lenta*, and five *L. tulipifera* trees. Random tree selection was performed (i.e., assigning numbers to all trees within the study area and randomly selecting numbers representing individual trees), but we also considered safety for tree and leaf access in our sampling design. *Fagus grandifolia* trees and *B. lenta* trees are shade tolerant and, thus, randomly selecting trees with ground-access leaves was possible even in the interior of the forest. *Liriodendron tulipifera* trees, however, are shade intolerant, forcing the *L. tulipifera* tree selection to be confined to near the forest edge where leaves were accessible from the ground. Trees with varying diameters (approximate range of 10–60 cm) were selected.

In situ temporal hyperspectral data collection

Hyperspectral measurements of leaves on the selected trees were acquired using a PSP-1100 Field-Portable Spectrophotometer (Spectral Evolution Inc., Lawrence, Massachusetts). This instrument measures the intensities of radiation at wavelengths from 320–1100 nm with a 1-nm resolution as a digital number and converts the intensities to percent reflectance using sensor-specific radiometric calibration. Nominal reference scans were taken before each measurement period using a calibrated white polytetrafluoroethylene plate (provided with the PSP-1100 by Spectral Evolution Inc). Reference scans were made using the same natural light conditions as the measurements and the instrument provided light source (i.e., 2 W tungsten halogen bulb). A 1-m-long bifurcated optical fiber connected the leaf clip to the PSP-1100. The integration time on the PSP-1100 is 7.5–2000 ms.

Measurements were taken from the beginning of August until abscission. The first set of hyperspectral measurements was taken on 05-Aug-2016 and the second on 01-Sept-2016. Between those days, one of the *F. grandifolia* trees was downed by a storm and had to be replaced by a different tree. After the second measurement day, measurements were taken every couple of days (usually between 2- and 4-day intervals with a couple slightly longer intervals due to weather conditions preventing measurements) until all leaves within reach on the tree had abscised. Measurements were taken on days with varying cloudiness levels on the



adaxial side of the leaves using a leaf clip that encloses the measured leaf section and uses its own light source (i.e., 2 W tungsten halogen bulb). Each time, five leaves per tree were measured. Measurements were taken in late afternoon within 2 h of sunset to try to minimize diurnal variation on the reflectance signatures. The number of days measured for each tree ranged from 20 to 27. In total, 1732 in situ hyperspectral reflectance measurements were taken.

Laboratory measurements

On the dates 05-Aug-2016, 03-Sept-2016, 18-Sept-2016, and 11-Oct-2016, we collected visibly green leaves from each of the selected trees for laboratory analyses. For each green leaf collection time, 15 F. grandifolia, 15 B. lenta, and 10 L. tulipifera leaves were collected. Based on when the lower-crown leaves in each tree were senescing, senescing leaves were collected from each tree on varying days. Eight to ten senescing leaves from each of the L. tulipifera trees were collected on 25-Oct-2016. Fifteen senescing leaves from each of the B. lenta trees were collected on 31-Oct-2016. Fifteen senescing leaves from each of the F. grandifolia trees were collected on 30-Oct-2016, 06-Nov-2016, 08-Nov-2016, or 11-Nov-2016, depending on the timing of senescence for a particular tree. Leaves were collected in paper bags and stored in the paper bags inside of plastic bags inside a cooler, transported to the laboratory within 2 h, and stored at 4 °C until the start of analyses.

Hyperspectral reflectance measurements were taken indoors within 2 h of collection on the adaxial side of each collected leaf using the same leaf clip and spectrophotometer as field measurements. Leaves were then briefly rinsed with Nanopure® deionized water and oven-dried at 70 °C for 72 h. Leaves were then ground up and stored in amber glass vials at 4 °C until N concentration measurements using a Vario EL cube (Elementar, Langenselbold, Germany). For each tree and collection date, ground samples were evenly mixed and 9.8–10.2 mg of the ground leaf matter was analyzed for N concentration.

Index selection and calculation

Based on a literature search, hyperspectral indices were selected that have been found to be correlated with different leaf traits that change during the autumn. Published indices are usually either highly specific and could be subject to overfitting or they fall into categories that use reflectances at similar wavelengths or the same mathematical form. By including several similar indices instead of just the most commonly used ones, we aimed to investigate how the explanatory power of different categories of indices compared to each other. Indices and their respective algorithms are provided in Table 1 where they are grouped by mathematical form. We highlight that

other studies (e.g., Serbin et al. 2014 and Barnes et al. 2017) have applied partial least squares regression to decompose the complete reflectance spectra and relate to plant traits, but we decided to limit the focus and scope of this study to previously published general indices for broader comparison and application of our results.

Data analysis

Linear regressions

Correlations between the selected hyperspectral indices and N concentrations in the collected leaves were investigated through fitting linear regressions of N concentration versus index value in a Bayesian framework. A Bayesian framework was selected because it allows for errors-in-variables (i.e., uncertainty in the index values) as well as observation uncertainty (i.e., in the N concentration measurements). Priors on the regression coefficients were given uninformative prior distributions of uniform (-100,100). We incorporated a normal data model with precision having a gamma (0.001, 0.0001) prior. To account for the errors in the independent variable (i.e., index measurements), means and precisions were calculated from the multiple leaves that were measured for each tree and collection time. We then incorporated these observation means and precisions in a normally distributed errors-in-variables model. Using the Markov Chain Monte Carlo in JAGS (Plummer 2003; version 4.3.0) called from R (R Core Team 2017; version 3.4.1) using the rjags (Plummer 2018; version 4.7) package, parameter posteriors were determined. All parameters converged and burn-in (Gelman-Brooks-Rubin values < 1.05) were removed. The five chains were run until the effective sample sizes for each parameter were > 5000. Models were compared using their deviance information criterion (DIC) values. To provide an analog model comparison to frequentist methods, adjusted correlation of determination (R^2) were calculated comparing the mean of the expected values for each posterior sample with the mean of the index values for each tree and collection number. The percentage of the posterior samples that were positive was also calculated for each model fit.

Phenology model fitting

Similar to the linear regressions performed on collected leaf data, autumn phenological curves were fit for each tree based on the different indices using a Bayesian framework. Models were fit using two approaches: linear regression (Eq. 1) and exponential (Eq. 2):

$$\mu_i = \beta_0 + \beta_1 \times t_i,\tag{1}$$

$$\mu_i = -a \times \exp(b \times t_i) + c + a, \tag{2}$$



Table 1 Mathematical forms of indices

Index	400s	500s	600s	700s	800s	References		
Normalized	differen	ce: (higher –	lower)/(highe	er + lower):				
PRI		531,570				Gamon et al. (1992)		
NDVI_H			680 800 1		Blackburn (1998)			
NDVI_M			619-671*		840-877*	Barnes et al. (2017)		
Car		530			800	Féret et al. (2011)		
Chl				712,780		Féret et al. (2011)		
NDRE				720,790		Fitzgerald et al. (2006)		
GNDVI		550		750		Gitelson and Merzlyak (1997)		
CCI**		526-536*	620-670*			Gamon et al. (2016)		
Modified no	ormalized	d difference: ((R750 - R705)	5)/(R750 - R705	$5+2\times R445$):			
mND	445			705,750		Sims and Gamon (2002)		
Spectra slop	e ratio: l	nigher/lower:						
RVI2		560			810	Xue et al. (2004)		
GM1		550		750		Gitelson and Merzlyak (1997)		
RVI1			660		810 Zhu et al. (2008)			
GM2				700,750		Gitelson and Merzlyak (1997)		
VGM				720,740		Vogelmann et al. (1993)		
LIC**	440		690			Lichtenthaler et al. (1996)		
RGI**		500-599*	600-699*			Multiple authors		
Modified sp	ectra slo	pe ratio: (R7:	50 – R445)/(F	R705 – R445):				
mSR	445			705,750		Sims and Gamon (2002)		
(R749 - R72)	20)/(R70	1 – R672):						
DD			672	701,720,749		le Maire et al. (2004)		
(R800 - R44)	45)/(R80	0 - R680):						
SIPI	445		680	Penuelas et al. (199		Penuelas et al. (1995)		
(R678 - R50)	00)/R750):						
PSRI		500	678	750		Merzlyak et al. (1999)		

Numbers indicate reflectance wavelengths (nm). Higher and lower indicate which wavelengths

where μ indicates the process-based modeled mean for the index value at different days of the year (t_i) . The priors on parameters β_0 and b were set as uniform (-100,100). The parameters controlling the direction of change, β_1 and a were modeled with most having a uniform (-100,0) parameter model. The indices PSRI, RGI, and SIPI, which are known to increase in the autumn instead of decrease like the other indices, were modeled with priors of uniform (0,100) on their β_0 and b parameters. The parameter c represents the index values at the start of the exponential growth/decay and, thus, represents expected index values for green leaves. Because of this, priors for the c parameter in each model fitting were more informed and taken from their respective references. If the references did not provide adequate examples of index values, priors were devised based on expected spectra relationships in green spectra (Sims and Gamon 2002). The parameter models for c were normally distributed and selected mean and standard deviations are provided in Table S1. All models had a normally distributed data model with the same precision prior as the models fit to N concentrations in collected leaves. Five chains were run, burn-in removed, and all parameters converged with effective sample sizes > 5000. Models were compared using their DIC values. Additionally, to give context on how the leaf collection dates correspond to landscape top-of-canopy phenological change, a double logistic curve was fit to MODIS NDVI product (MODIS13Q1; Didan 2015) values for 1 year (1 July 2016 to 30 June 2017) using the logistic equation from Zhang et al. (2003).

Results

In the comprehensive models, which include all measured leaves, all indices were able to determine slopes significantly different from zero (>95% of their posterior; Table 2). Additionally, we found that the reflectance values at the wavelengths 445 nm and 440 nm (blue/violet) increased significantly (>95% of the posterior slope samples were positive) in 11 of the 15 trees throughout



^{*}Averaged. **Lower and higher switched in equation

 Table 2
 Diagnostic

 characteristics for the different
 indices

Index	All	Green 1	Green 2	Green 3	Green 4	Senescing	R^2	DIC
Chl	1.00	0.70	0.82	0.83	1.00	1.00	0.86	-31.12
NDVI_H	1.00	0.78	0.97	0.88	0.99	0.99	0.85	-24.12
NDVI_M	1.00	0.75	0.96	0.84	1.00	1.00	0.85	-21.23
NDRE	1.00	0.46	0.86	0.85	1.00	1.00	0.84	-18.53
GM2	1.00	0.90	0.77	0.93	1.00	0.97	0.83	-15.33
mND	1.00	0.52	0.47	0.40	0.88	0.99	0.82	-8.27
PSRI	0.00	0.58	0.07	0.85	0.77	0.22	0.77	7.41
RGI	0.00	0.38	0.39	0.49	0.03	0.96	0.76	10.62
GNDVI	1.00	0.83	0.99	0.96	1.00	1.00	0.77	17.34
CCI	0.00	0.40	0.51	0.39	0.01	0.97	0.75	12.23
DD	1.00	0.84	0.31	0.60	0.94	0.38	0.72	22.51
mSR	1.00	0.48	0.12	0.40	0.85	0.96	0.72	22.59
PRI	1.00	0.44	0.22	0.20	0.99	0.09	0.72	23.54
RVI2	1.00	0.81	0.99	0.97	1.00	1.00	0.71	24.44
GM1	1.00	0.83	0.98	0.98	1.00	1.00	0.70	27.49
RVI1	1.00	0.70	0.84	0.91	1.00	0.99	0.66	38.30
SIPI	0.00	0.25	0.01	0.74	0.35	0.03	0.65	39.26
VGM	1.00	0.51	0.39	0.65	0.98	0.75	0.80	48.37
Car	1.00	0.84	1.00	0.96	1.00	1.00	0.65	53.38
LIC	1.00	0.41	0.20	0.18	0.11	0.01	0.33	87.42

The columns all through senescing indicate the fraction of posterior samples that have a positive slope. Italicized numbers in those columns indicate models that have a significant trend (i.e., > 95% or < 5% of the posterior samples had a positive slope). Adjusted R^2 and DIC (deviance information criterion) values for each index with N concentration across all collected leaves are given in the last two columns

autumn. Chl, the two NDVI indices, and NDRE were the strongest predictors of leaf N concentration for the comprehensive models (i.e., models fit to data from all collected leaves; Table 2).

Based on the MODIS fit, the third green collection (18-Sept) occurred around the senescence-onset date of

the top-of-canopy leaves and the fourth green collection occurred when the top-of-canopy leaves had already started senescing (Fig. 1). Indices that included similar wavelengths (Fig. 2) were usually able to detect significant trends in the same collections. None of the indices were able to determine a statistically significant slope for the first green collection

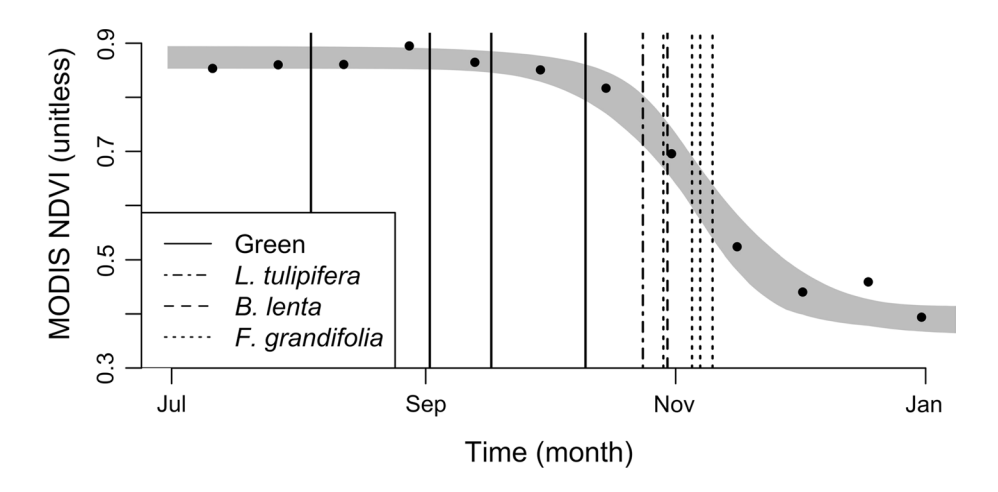
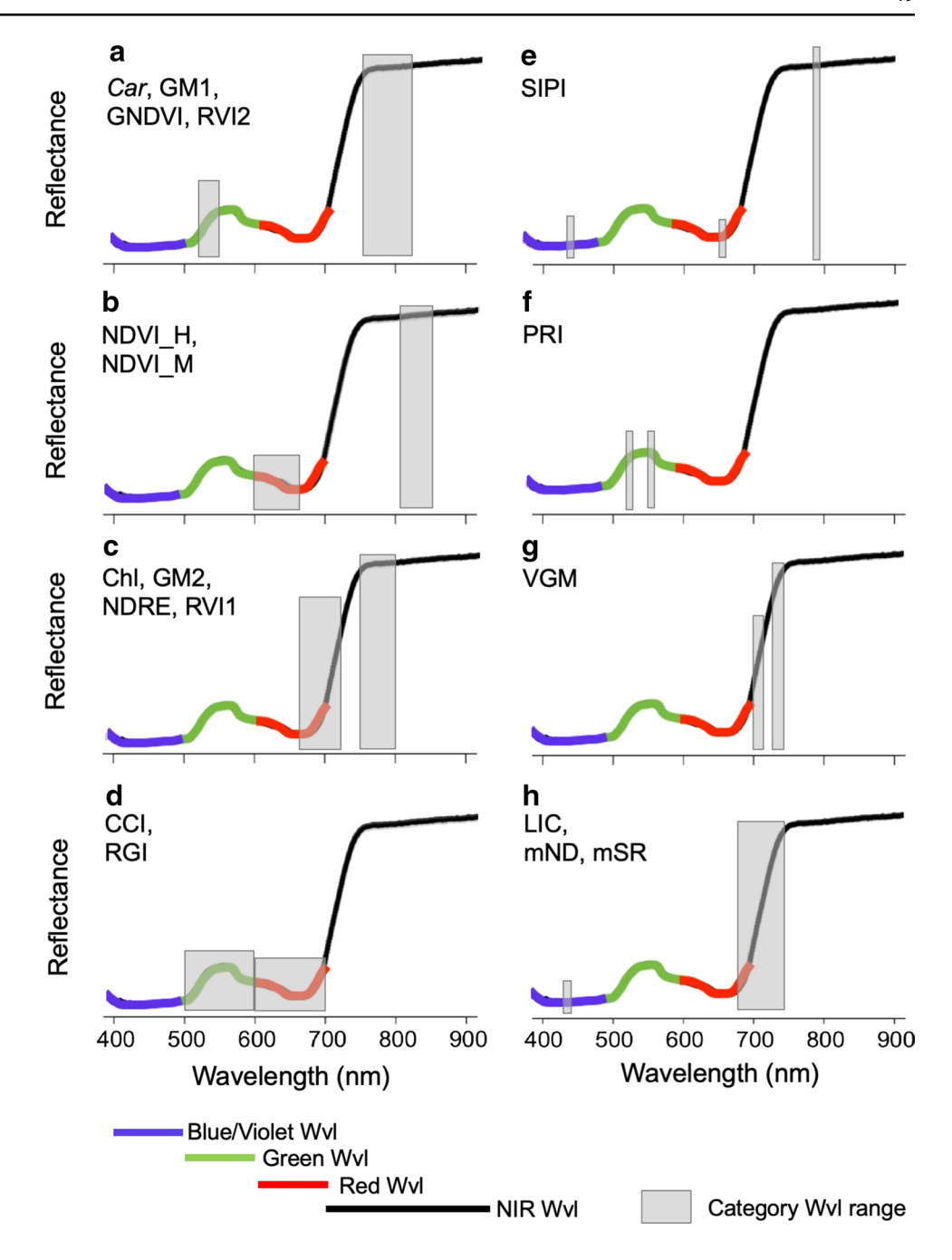


Fig. 1 Autumn phenological curve fit of MODIS data. The MODIS NDVI values are given in the black dots with the 95% credible interval for the curve indicated by the shading. The solid vertical lines indicate the four dates when lower-crown green leaves were collected from *Fagus grandifolia* Ehrh., *Liriodendron tulipifera* L., and *Bet*-

ula lenta L. trees. The dotted vertical lines indicate the dates when senescing leaves were collected from the respective tree species. The fourth green collection occurred when the upper-canopy leaves had just started senescing



Fig. 2 Selected indices grouped by similar included wavelengths ranges, which are indicated by the gray boxes. For reference, approximate locations of violet/blue (400 nm range), green (500 nm range), and red (600 nm range) wavelength (wvl) ranges are colored on each plot. Near-infrared (NIR) is shown in black. These are given to improve the understanding of what each index measures (e.g., a and d show indices that include one reflectance that is appears approximately green). a Indices with green and NIR wavelengths. b Indices with short red and NIR wavelengths. c Indices with long red and NIR wavelengths. d Indices with green and red wavelengths. e Index with blue/violet, red, and NIR wavelengths. f Index with two green wavelengths. g Index with two wavelengths along the red-edge. h Indices with a blue/ violet wavelength and one along the red-edge. Throughout the analysis, the performance of the indices grouped by the wavelengths used and not the form of their mathematical forms (color figure online)



(Table 2). The indices associated with the red edge and the green wavelengths along with SIPI, NDVI_H, and NDVI_M were able to determine significant trend with leaf N concentrations (Table 2). The poor DIC scores and low adjusted R^2 values (all below 0.2) for the first three green collections (Aug and both in Sept) indicated that all indices lacked any explanatory and predictive power for N concentrations and, thus, they are not provided here. The indices associated with only the red edge were able to determine significant trends in the fourth green collection (14-Oct) and the senescing collection. PRI and VGM were able to determine a trend in the fourth green collection and mSR, mND, and LIC were able

to in the senescing collection. The fourth green collection had the most indices that were able to determine significant slopes. Both the fourth green and senescing collections had indices that were able to explain over half of the variance in leaf N concentration (Table 3). For most of the indices, the credible interval (CI) and predictive interval (PI) for the fourth green collection did not include the mean observations in the senescing collection and vice versa, indicating that the models fit to the green and senescing collections have no predictive power for leaves in the other collection. The NDVI, PRI, and NDRE fits for the fourth green collection included the means in the senescing collection (Fig. 3).



Table 3 Adjusted R^2 and DIC (deviance information criterion) values for the fourth green and the senescing collections (N% vs. index)

Index	Fourth Gr	een	Senescing	
GM2	0.61	-14.15	0.31	-22.05
GM1	0.53	-11.29	0.63	-31.18
GNDVI	0.51	-11.25	0.69	-33.55
RVI2	0.52	-10.85	0.60	-29.96
Chl	0.48	-9.90	0.42	-24.48
NDVI_M	0.45	-9.80	0.44	-25.01
RVI1	0.44	-8.64	0.32	-22.02
Car	0.41	-8.61	0.71	-34.84
NDVI_H	0.38	-7.93	0.29	-21.41
NDRE	0.40	-7.69	0.4	-23.92
VGM	0.49	-7.03	0.37	-17.98
PRI	0.30	-5.38	0.06	-17.23
RGI	0.17	-2.78	0.18	-19.75
CCI	0.27	-8.134	0.18	-22.73
DD	0.12	-1.83	-0.07	-15.23
LIC	0.05	-0.66	0.27	-21.03
mND	0.03	-0.51	0.27	-21.00
mSR	0.01	-0.09	0.25	-20.96
SIPI	-0.08	0.40	0.17	-19.08
PSRI	-0.03	0.58	-0.03	-15.85

Italicized numbers indicate R^2 values greater than 0.50

The RVI1, and mSR senescing fits included the means in the fourth green collection. Chl and GM2 fourth green models including the senescing means and vice versa (Fig. 3). GM2 had a better DIC value than Chl in the fourth green collection, but they had similar DIC values in the senescing collection. The CI for the senescing Chl fit was much tighter than that of the senescing GM2 fit (Fig. 3). The variance in the N concentrations for each collection, in order, was 0.028, 0.086, 0.041, 0.043, and 0.014.

Overall, linear fits for most indices had lower DIC values than exponential fits for the in situ autumn phenology curves (Table 4). Based on DIC values of the models between the indices and the in situ reflectance measurements, there was some variation between trees on the strongest indicator of phenology, but NDRE and PRI were the top two strongest indicators in all but one tree. The top four indices (e.g., NDRE, PRI, CCI, and Chl) were consistent among all trees (Table 4). The indices NDVI_M and NDVI_H had similar middle ranking for all trees (Table S2). NDRE and Chl were among the best at tracking autumn phenological progression and predicting N. The NDVI (i.e., NDVI_M and NDVI_H) values were stronger predictors for N concentrations, but did not represent the autumn phenological changes as distinctly as many of the other indices (e.g., NDRE, PRI, and Chl).

The indices PRI and CCI had a very strong phenological signal, but was a poor predictor of N overall.

Discussion

Increasing correlations between indices and N throughout autumn

The N concentration in leaves is fundamental to many tree and ecosystem processes, both while the leaves are still attached and after they have abscised. Thus, it is important to be able to monitor leaf N, especially in relatively inexpensive, non-destructive ways, such as using hyperspectral indices within the visible and NIR ranges. As expected, none of the indices had any explanatory power (weak R^2 and DIC values) for the first three green collections (Aug and both Sept dates), but some indices that had been previously found to be correlated with chlorophyll concentrations had some explanatory power (four indices had R^2 values greater than 0.50) in the fourth green collection (14-Oct) and the senescing collection. The increase in the correlation between the chlorophyll-based indices and N in the fourth green and the senescing collections is as expected due to N resorption. While Croft et al. (2017) found that ratios between N and chlorophyll dropped at the end of the season, this should only occur if enough of the chlorophyll had been resorbed to increase the weight of the cell structure associated N. Our senescing leaves likely had not reached this stage yet because explanatory power remained, but one should be mindful of this in measuring senescing leaves that have undergone high levels of N resorption already. While the leaves in the fourth green collection were still green, they were collected after phenological change in the top-of-canopy was evident from MODIS. Thus, even though this study did not focus on how to scale its results to larger monitoring efforts, top-of-canopy remote sensing can be an adequate way to identify when these indices could have explanatory power in lower-crown leaves; however, lower-canopy studies are still uncommon and the linkage between low- and high-canopy leaves still needs to be addressed.

The degree of explanatory power of the indices for the different collections was more similar amongst indices that included similar wavelengths (Fig. 2) and not by mathematical form (Table 1). Because this study was focused on the power to explain N concentrations, we did not measure pigment concentrations. While the lack of pigment data for the actual leaves measured is a limitation of this study, there have been extensive previous studies that have found correlations between the indices and pigment concentrations (i.e., chlorophyll and carotenoid concentrations and ratios). The



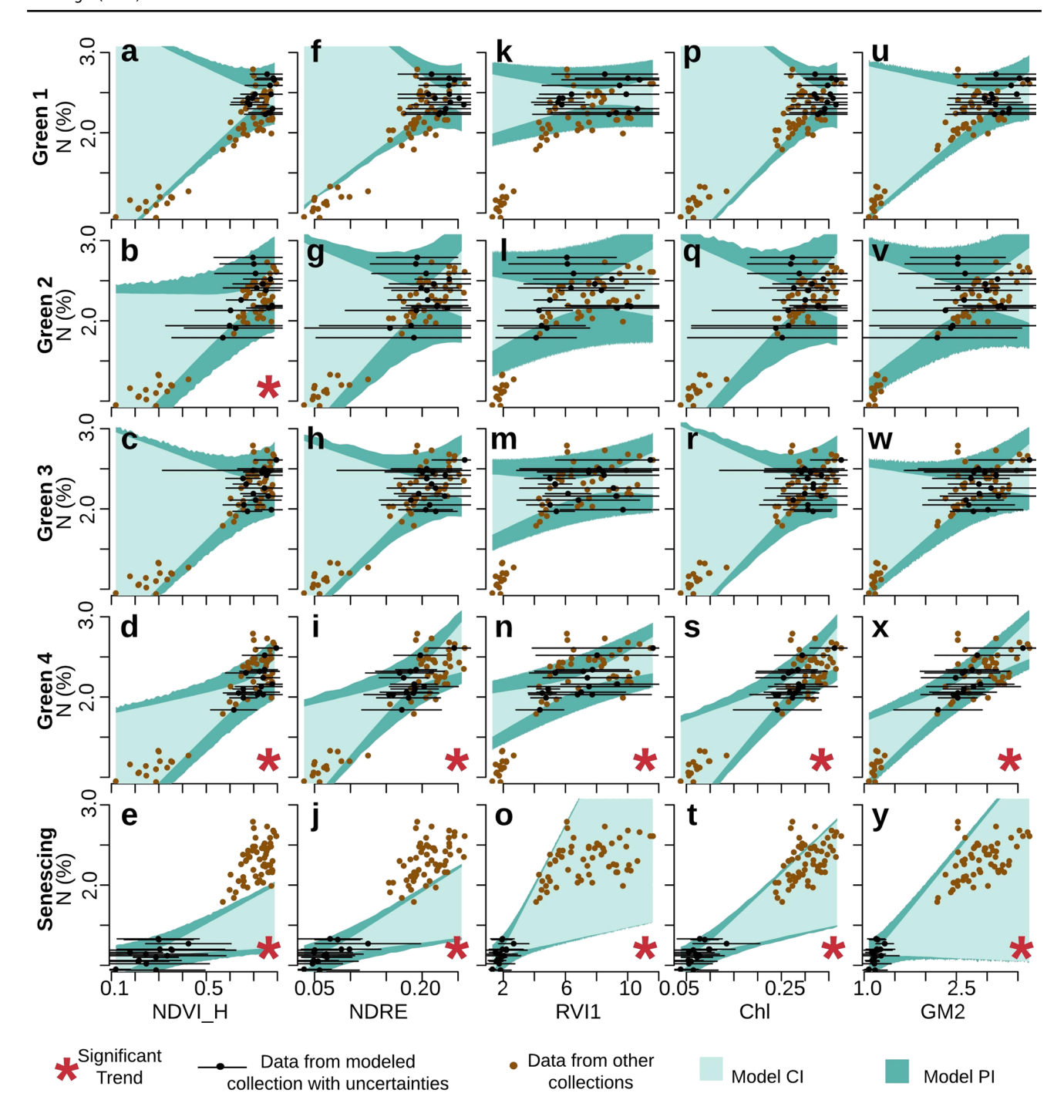


Fig. 3 Selected collected model fits for individual collections. First column is NDVI_H for green 1–4 and senescing collections (panels a–e, respectively). Second column is NDRE for green 1–4 and senescing collections (f–j, respectively). Third column is RVII for green 1–4 and senescing collections (k–o, respectively). Fourth column is Chl for green 1–4 and senescing collections (p–t, respectively). Fifth column is GM2 for green 1–4 and senescing collections (u–y, respectively). The darker shading indicates the 95% predictive interval (PI) and the lighter shading indicates the 95% credible interval (CI). The black points indicate the measurements for that specific collection, which is indicated for each row on the left. The black horizontal lines give the 95% confidence interval for the index

values. The brown/lighter gray points without horizonal lines indicate the measurements for other collections. The PI and CI for models fit to some collection numbers do not always include measurements from other collections and no indices were able to determine a significant trend in the first green (indices with significant trends in the third green not shown). While diagnostic statistics for model performance were relatively strong in the green four and senescing collections, the green 4 models often included the senescing data within their PI, but the senescing models rarely included the other collections within their PI. The green 4 and senescing models for Chl and GM2 included data from the other collections within their PI (color figure online)



Table 4 The DIC values of the top six in situ phenology fits for each tree (five trees per species)

Model	DIC	Model	DIC	Model	DIC	Model	DIC	Model	DIC
F. grandifolia									
$NDRE^{L}$	-497.1	$NDRE^{L}$	-505.1	$NDRE^L$	-400.4	$NDRE^{L}$	-432.4	$NDRE^{L}$	-441.3
$NDRE^{E}$	-410.9	$NDRE^{E}$	-414.5	$NDRE^{E}$	-305.2	$NDRE^{E}$	-375.2	PRI^{L}	-358.9
PRI^{L}	-399.9	PRI^{L}	-376.2	CCI^L	-293.1	PRI^{E}	-375.2	CCI^L	-344.5
PRI^{E}	-397.8	CCI^L	-371.1	Chl^L	-290	$PSRI^{E}$	-346.8	$NDRE^{E}$	-341.8
CCI^L	-376.5	Chl^L	-368.1	Car ^L	-286.9	Chl^E	-344.1	Chl^L	-341.4
Chl^L	-373.5	Car^{L}	-367	$GNDVI^{L}$	-276.1	PRI^{L}	-342.5	Car^{L}	-328.8
B. lenta									
$NDRE^{L}$	-473	PRI^{L}	-424.7	PRI^{E}	-399	PRI^{L}	-355.1	$NDRE^{L}$	-424.7
PRI^{L}	-419	$NDRE^{L}$	-418.7	PRI^{L}	-396	$NDRE^{L}$	-351.5	PRI^{L}	-390
PRI^{E}	-403.3	$NDRE^{E}$	-336.4	$NDRE^{L}$	-381.9	PRI^{E}	-297.9	PRI^{E}	-352.1
$NDRE^{E}$	-398	CCI^L	-330.3	$NDRE^{E}$	-338.6	$NDRE^{E}$	-288.2	$NDRE^{E}$	-345.5
Chl^{E}	-367.9	Chl^L	-327.3	$PSRI^{E}$	-310.4	CCI^L	-265.4	CCI^L	-331.7
CCI^L	-365	Chl^E	-308.4	Chl^{E}	-309.4	Chl^L	-262.4	Chl^L	-328.6
L. tulipifera									
PRI^{L}	-374.7	PRI^{L}	-335.9	PRI^{L}	-395.6	PRI^{L}	-346.9	$NDRE^{L}$	-351.4
$NDRE^{L}$	-330	$NDRE^{L}$	-317	$NDRE^{L}$	-335.3	$NDRE^{L}$	-312.6	PRI^{L}	-350.1
$NDRE^{E}$	-276.3	PRI^{E}	-265.3	PRI^{E}	-304.2	PRI^{E}	-280.8	CCI^{L}	-280.7
CCI^L	-244.8	$NDRE^{E}$	-260.8	$NDRE^{E}$	-279.2	$NDRE^{E}$	-266.6	Chl^L	-277.7
Chl^L	-241.8	CCI^L	-232.7	CCI^L	-247.2	CCI^L	-228.5	$NDRE^{E}$	-276.1
$PSRI^{L}$	-229.1	Chl^L	-229.7	Chl ^L	-244.1	Chl^L	-225.4	PRI^{E}	-273.6

^LIndicates the linear regression fit and ^Eindicates the exponential fit

behaviors of the explanatory power of N concentrations for the indices follow the understanding that previous studies have gained on the correlations of indices with pigment and autumnal pigment change.

The indices that included one wavelength above 750 nm (NIR) and one around 550 nm (green; GM1, GNDVI, RVI2; Fig. 2a) had R^2 values over 0.50 for both the fourth green and the senescing collections models, with higher values in the senescing collection. Chlorophyll reflects green light in the 550 nm region and by including both a wavelength in this region and another either within the red-edge or above it, these indices appear to be able to have the strongest ability to monitor N resorption and N concentrations. Their predictive ability was strongest in the senescing collection likely because even though the senescing collection had the lowest variance in N concentrations, the variance in the senescing collection was likely due to differences in the degree of N resorption instead of inherent differences in how the different trees allocate N. Additionally, by including wavelengths in both the green region and around the red edge, these indices appear to perhaps enhance the differences between the leaves even though the N variation was low. In contrast, GM2 had the strongest explanatory and predictive power (based on its DIC and adjusted R^2 values) for the fourth green collection, but had much lower explanatory power in the senescing collection. GM2 only included wavelengths along the red edge and perhaps the N variance in the senescing collection was not great enough to produce a higher correlation. The 550-560 nm (green) range was important at allowing for the stronger explanatory power because the index Car behaved differently. Car also has a wavelength within the same upper region, but has a lower wavelength of 530 nm, which is below the green peak in the spectra (Fig. 2a). The Car index has been found to be highly sensitive to carotenoid concentrations (Féret et al. 2011). Because N is not resorbed from the breakdown of carotenoids, this high correlation between Car and N concentrations in the senescing collection is likely due to measuring the phenological state of the progressions of carotenoid breakdown and N resorption. Indices that included a wavelength above 750 nm (NIR) and one around 550-560 nm (green) had high explanatory power within the fourth green and senescing collections, but by replacing the lower wavelength with 530 nm more explanatory power was achieved in the senescing collection and substantially less in the fourth green collection.

Changes in relationships throughout autumn

Even though GM1, GNDVI, and RVI2 had among the highest explanatory powers for both the fourth green (14-Oct) and senescing collections, the models they fit between the two green collections were vastly different and did not include the means of the other collection within their predictive intervals. With the exception



of Chl and GM2, none of the indices fit models for the fourth green and senescing collections that included the means of the other collection within their PI. Even though it did not produce the strongest DIC and R^2 values, Chl created the most consistent models between the fourth green and senescing collections. Thus, the index Chl was the least sensitive to phenophase in the time right before and into senescence. Regression models fit using any of the other indices are likely to be highly specific to the phenophase of collection and are not as able to predict N concentrations in the other phenophase (i.e., the time right before senescence or senescence). The importance of phenophase in determining leaf trait relationships has been shown before for green leaves (McKown et al. 2013), but is still not considered enough in trait spectra relationship studies. This needs to be considered for more leaf-trait/leaf-trait and leaf-trait/spectra relationships, especially if they are related to leaf traits that have a phenological change.

Earlier detections in trends

While all of the indices had virtually no explanatory and predictive power for the first three green collections, the indices that included one wavelength in the 500s (green) and one above 750 nm (NIR; RVI2, GM1, GNDVI, and Car; Fig. 2a) were able to determine significant trends for the second and third green collections and likely possess the most potential for measuring the start of the autumn phenological transition period (Fig. 4). Later in the summer, deciduous trees switch from expressing senescence down-regulated genes to senescence-associated genes (Taiz and Zeiger 2006). Chloroplasts are the first organelle to start to break down (Keech et al. 2007), with chlorophyll and carotenoids decreasing with similar rates (García-Plazaola et al. 2003). Since we did not collect any pigment data, we can only postulate that our second and third green collections occurred at this time (Fig. 4) where the chlorophyll and carotenoids are decreasing in similar amounts. The indices that were able

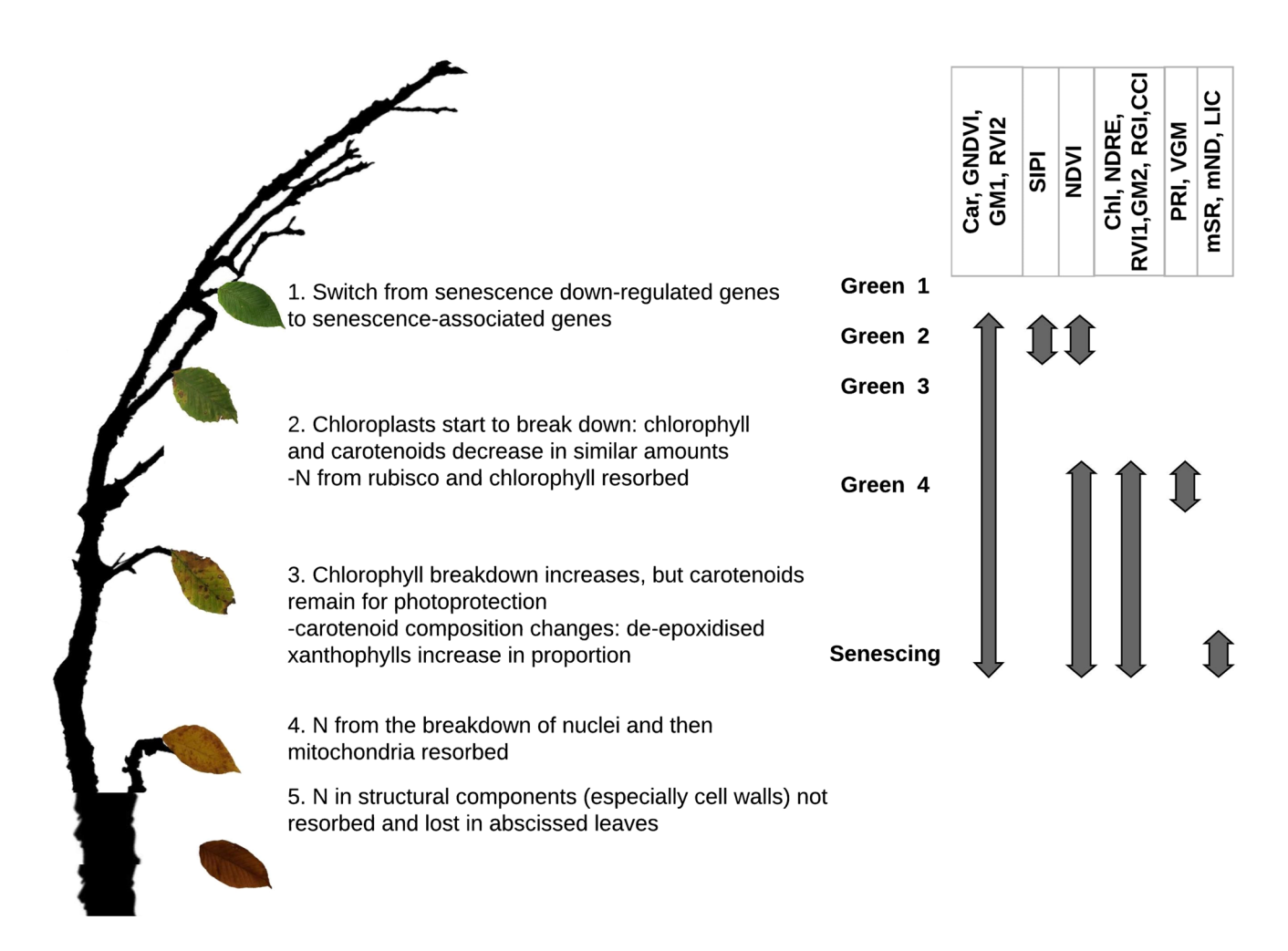


Fig. 4 Seasonal shift in the abilities of the indices to detect significant trends and likely respective physiological changes. The gray vertical arrows indicate when the respective indices were able to detect a significant trends and likely respective physiological changes.

nificant trend with respect to potential physiological changes (color figure online)



to determine the direction of the relationship during both of these collections only included the indices that had wavelengths both near and above the red edge and near the green portion of the visible spectra. These wavelengths are known to give information about chlorophyll and carotenoid concentrations because of their inherent reflectance and absorption properties. By including both, it appears like they might have been able to amplify the effect that the breakdown of both chlorophyll and the carotenoids have on N concentration, even though carotenoids do not contain N. In the green region, chlorophyll reflects light and the carotenoids absorb it. Decreasing chlorophyll concentrations will not affect the amount that is reflected due to chlorophyll, but decreasing carotenoid concentrations will affect the amount of green light that is being absorbed by the leaf. Chlorophyll is likely not decreasing enough at this point to allow the indices that focus only on that pigment to detect differences in N concentration, but it appears that likely by detecting the additive changes in both types of pigments these indices are able to detect the sign of the slope of correlation with N concentrations. These indices were also some of the best at explaining variation in N concentrations in the fourth green (14-Oct) and senescing collections, likely for similar reasons. While further work should be done with pigment data to investigate our postulation of the physiological cause, we found that the wavelengths with one wavelength in the 500s (green) and one above 750 nm (NIR) were the first to be able to detect a significant trend with N concentrations.

Patterns in indices modified for differences in high leaf surface reflectances

Indices with a wavelength in the 400 nm (blue/violet) range (mSR, mND, and LIC) have been previously found to have strong correlations with N concentrations in green, sunlit leaves (e.g., Sims and Gamon 2002), but were found here to have weak correlations with lower-crown leaves in all green collection models. These indices only had a significant trend with N concentrations in the senescing collection. Sims and Gamon (2002) created the indices mND and mSR by adding a third reflectance at wavelength 445 nm to a normalized difference and a simple slope ratio, respectively, to compensate for high leaf surface reflectance where the entire spectrum is raised. They note, though, that R445 only remains constant until the total chlorophyll drops to a low level. However, we found that these wavelengths increased in the majority of the measured trees in the autumn indicating that they have a different impact than just correcting for high leaf surface reflectances. Modifying the indices with the reflectance at 445 nm likely partially masked the changes in the other regions with gradual chlorophyll breakdown in the green collections. But, these indices were able to detect trends in the senescing collection (with adjusted R^2 values between 0.25 and 0.27) likely because the reflectance at these wavelengths also changed with much lower chlorophyll concentrations, reinforcing the relationship between chlorophyll and N concentrations and widening the chlorophyll measurement ability. Modifying indices by including a reflectance in the 400s weakens the ability of the index to rely on the phenological change of resorption to identify trends in N concentrations.

Strong correlations overall and relations with phenological change

We have shown that across the autumn phenological transition, some hyperspectral indices in the visible and NIR wavelengths are able to predict N concentrations in lowercrown leaves, with the indices Chl, NDVI_H, NDVI_M, and NDRE having the strongest explanatory power. These abilities seem to be physiologically based because they are not necessarily the same as the ones that had the most consistent phenological change. Contrary to expectations, the NDVI indices (i.e., NDVI_H and NDVI_M) were not the strongest indicators of phenological change compared to many of the other indices. NDVI is one of the major metrics for canopy-level phenological change, but perhaps at least on the leaf level other metrics could be more informative. Even though PRI and CCI were strong indicators of autumn phenological change, they were poor predictors of N concentrations overall. Dillen et al. (2012) also found that PRI was a good indicator of leaf physiological change and found it to be less correlated with photosynthesis-related traits than indices that focus on the red edge. PRI has been shown to be sensitive to changes in the xanthophyll cycle diurnally (Gamon et al. 1992; Van Gaalen et al. 2007), carotenoid to chlorophyll concentrations seasonally (Sims and Gamon 2002; Stylinksi et al. 2002; Hilker et al. 2011), and levels of water stress (Peguero-Pina et al. 2008). The index CCI has been found to be a strong tracker of photosynthetic phenology in evergreen conifers (Gamon et al. 2016). We also found it to be a strong, consistent tracker of phenological change in deciduous leaves even though it had a weaker correlation than many others with N concentrations across and within collections. Since NDRE and PRI measure changes in different pigments, deciding which one to utilize would depend on the application. For example, monitoring the breakdown of chlorophyll and N resorption, NDRE or Chl (or an ensemble) would be more applicable, but PRI would be more suitable to monitoring changes to the carotenoids. Because the indices performed similarly across all trees, our results should not be sensitive to tree selection. These indices are appropriate to use to synchronize other leaf trait relationships by phenological progression.



Conclusions

Leaf N is fundamental in numerous physiological and ecosystem processes. Hyperspectral indices have been shown to be able to predict N concentrations by measuring the reflectance at wavelengths in the visible through SWIR wavelengths; however, instruments that allow for the measuring of SWIR are substantially more expensive than instruments that are limited to the visible and NIR range. We have shown that while published indices in the visible and NIR are not able to reliably detect trends in N in midsummer lowercrown leaves, autumn phenological changes allow for an increase in the explanatory power of many indices. Indices that include wavelengths in the upper-green (550–560 nm) and NIR were able to detect significant trends with leaf N earliest (in Sept) and could serve as indicators of the first stages of this transition. We also found that most of these indices (GM1, GNDVI, and RVI2) were able to explain over half of the variation in leaf N in lower-crown green leaves collected after the crowns had started senescing and in lower-crown senescing leaves. The indices GM2 and Car explained the most variation in N in the last green and senescing collections, respectively. Almost all of the models differed between the last green and senescing collections, with the exceptions of Chl and GM2. Thus, while correlations may be higher for some indices (GM1, GNDVI, and RVI2), their models are more reliant on ensuring the leaves are in the same phenophase.

The index Chl was found to explain the most variation in N concentrations across the autumn phenological change and, along with PRI, NDRE, and CCI, was one of the strongest indicators of this progression. NDRE was also strongly correlated with N overall, but PRI and CCI were less correlated and had poor predictive power. We also show that not only is it necessary to consider phenology, but that it can allow for the development of trait relationships that are useful in the near-remote sensing of N concentrations. In a way, the parallel autumn breakdown of chloroplasts and N resorption, which is known to happen in most deciduous trees, potentially provides a way for leaf economic principles to be applied to lower-crown, shaded leaves and should be investigated for additional traits.

Acknowledgements This work was funded through the University of Delaware's research office. We thank Fair Hill Natural Resource Management Area for graciously providing a location for data collection. We also thank Gerald Poirier, Janice Hudson, Kalmia Kniel, and Alexey Shiklomanov for useful advice during the project. KW also acknowledges support under the National Science Foundation Graduate Research Fellowship (1247312). RV acknowledges support from NASA Carbon Monitoring Systems (80NSSC18K0173) and the National Science Foundation (1652594). Hyperspectral data and leaf trait measurements are available on EcoSis.org (https://ecosis.org/package/spectra-from-insitu-deciduous-leaves-and-leaves-collected-for-nitrogen-analy sis-throughout-autumn).

Author contribution statement KW, DL, and RV conceived and designed the experiments. KW performed the experiments and analyzed the data. KW wrote the manuscript with input and edits from DL and RV. KW, DL, and RV worked on manuscript revisions.

References

- Barnes ML, Breshears DD, Law DJ, van Leeuwen WJD, Monson RK, Fojtik AC, Barron-Gafford GA, Moore DJP (2017) Beyond greenness: Detecting temporal changes in photosynthetic capacity with hyperspectral reflectance data. PLoS One 12:e0189539. https:// doi.org/10.1371/journal.pone.0189539
- Berg B, McClaugherty C (2003) Plant litter. Decomposition, humus formation, carbon sequestration. Springer, Berlin, p 286
- Berg B, Meentemeyer V (2002) Litter quality in a north European transect versus carbon storage potential. Plant Soil 242:83–92
- Blackburn GA (1998) Quantifying chlorophylls and carotenoids at leaf and canopy scales: an evaluation of some hyperspectral approaches. Remote Sens Environ 66:273–285
- Chapin FS, Kedrowski RA (1983) Seasonal changes in nitrogen and phosphorus fractions and autumn retranslocation in evergreen and deciduous Taiga Trees. Ecology 64:376–391. https://doi.org/10.2307/1937083
- Croft H, Chen JM, Luo X, Bartlett P, Chen B, Staebler RM (2017) Leaf chlorophyll content as a proxy for leaf photosynthetic capacity. Glob Change Biol 23:3513–3524. https://doi.org/10.1111/gcb.13599
- Didan K (2015) MOD13Q1 MODIS/Terra Vegetation Indices 16-Day L3 Global 250 m SIN Grid V006 [NDVI and pixel_reliability]. NASA EOSDIS LP DAAC. https://doi.org/10.5067/modis/mod13 q1.006
- Dillen SY, de Beeck MO, Hufkens K, Buonanduci M, Phillips NG (2012) Seasonal patterns of foliar reflectance in relation to photosynthetic capacity and color index in two co-occurring tree species, *Quercus rubra* and *Betula papyrifera*. Agric For Meteorol 160:60–68. https://doi.org/10.1016/j.agrformet.2012.03.001
- Estiarte M, Peñuelas J (2015) Alteration of the phenology of leaf senescence and fall in winter deciduous species by climate change: effects on nutrient proficiency. Glob Change Biol 21:1005–1017. https://doi.org/10.1111/gcb.12804
- Féret J-B, François C, Gitelson A, Asner GP, Barry KM, Panigada C, Richardson AD, Jacquemoud S (2011) Optimizing spectral indices and chemometric analysis of leaf chemical properties using radiative transfer modeling. Remote Sens Environ 115:2742–2750. https://doi.org/10.1016/j.rse.2011.06.016
- Fitzgerald GJ, Rodriguez D, Christensen LK, Belford R, Sadras VO, Clarke TR (2006) Spectral and thermal sensing for nitrogen and water status in rainfed and irrigated wheat environments. Precis Agric 7:233–248. https://doi.org/10.1007/s11119-006-9011-z
- Gallinat AS, Primack RB, Wagner DL (2015) Autumn, the neglected season in climate change research. Trends Ecol Evol 30:169–176. https://doi.org/10.1016/j.tree.2015.01.004
- Gamon JA, Peñuelas J, Field CB (1992) A narrow-waveband spectral index that tracks diurnal changes in photosynthetic efficiency. Remote Sens Environ 41:35–44. https://doi.org/10.1016/0034-4257(92)90059-S
- Gamon JA, Huemmrich KF, Wong CYS, Ensminger I, Garrity S, Hollinger DY, Noormets A, Peñuelas J (2016) A remotely sensed pigment index reveals photosynthetic phenology in evergreen conifers. Proc Natl Acad Sci 113(46):13087–13092. https://doi.org/10.1073/pnas.1606162113



García-Plazaola JI, Hernández A, Becerril JM (2003) Antioxidant and pigment composition during autumnal leaf senescence in woody deciduous species differing in their ecological traits. Plant Biol 5:557–566. https://doi.org/10.1055/s-2003-44791

- Gill AL, Gallinat AS, Sanders-DeMott R, Rigden AJ, Gianotti DJS, Mantooth JA, Templer PH (2015) Changes in autumn senescence in northern hemisphere deciduous trees: a meta-analysis of autumn phenology studies. Ann Bot 116:875–888. https://doi. org/10.1093/aob/mcv055
- Gitelson AA, Merzlyak MN (1997) Remote estimation of chlorophyll content in higher plant leaves. Int J Remote Sens 18:2691–2697. https://doi.org/10.1080/014311697217558
- Hikosaka K (2016) Optimality of nitrogen distribution among leaves in plant canopies. J Plant Res 129:299–311. https://doi.org/10.1007/ s10265-016-0824-1
- Hilker T, Gitelson A, Coops NC, Hall FG, Black TA (2011) Tracking plant physiological properties from the multi-angular tower-based remote sensing. Oecologia 165:865–876
- Homolová L, Malenovský Z, Clevers JGPW, García-Santos G, Schaepman ME (2013) Review of optical-based remote sensing for plant trait mapping. Ecol Complex 15:1–16. https://doi.org/10.1016/j.ecocom.2013.06.003
- Inagaki Y, Miura S, Kohzu A (2004) Effects of forest type and stand age on litterfall quality and soil N dynamics in Shikoku district, southern Japan. For Ecol Manag 202:107–117. https://doi.org/10.1016/j.foreco.2004.07.029
- Inagaki Y, Okuda S, Sakai A, Nakanishi A, Shibata S, Fukata H (2010) Leaf-litter nitrogen concentration in hinoki cypress forests in relation to the time of leaf fall under different climatic conditions in Japan. Ecol Res 25:429–438. https://doi.org/10.1007/s11284-009-0672-8
- Keech O, Pesquet E, Ahad A, Askne A, Nordvall D, Vodnala SM, Tuominen H, Hurry V, Dizengremel P, Gardeström P (2007) The different fates of mitochondria and chloroplasts during darkinduced senescence in Arabidopsis leaves. Plant, Cell Environ 30:1523–1534. https://doi.org/10.1111/j.1365-3040.2007.01724.x
- Keenan TF, Niinemets Ü (2016) Global leaf trait estimates biased due to plasticity in the shade. Nat Plants 3:16201. https://doi.org/10.1038/nplants.2016.201
- Keenan TF, Gray J, Friedl MA, Toomey M, Bohrer G, Hollinger DY, Munger JW, O'Keefe J, Schmid HP, Wing IS, Yang B, Richardson AD (2014) Net carbon uptake has increased through warminginduced changes in temperate forest phenology. Nat Clim Change 4:598–604. https://doi.org/10.1038/nclimate2253
- le Maire G, François C, Dufrêne E (2004) Towards universal broad leaf chlorophyll indices using PROSPECT simulated database and hyperspectral reflectance measurements. Remote Sens Environ 89:1–28. https://doi.org/10.1016/j.rse.2003.09.004
- LeBauer DS, Treseder KK (2008) Nitrogen limitation of net primary productivity in terrestrial ecosystems is globally distributed. Ecology 89:371–379. https://doi.org/10.1890/06-2057.1
- Lichtenthaler HK, Lang M, Sowinska M, Heisel F, Miehé JA (1996)
 Detection of vegetation stress via a new high resolution fluorescence imaging system. J Plant Physiol 148:599–612. https://doi.org/10.1016/S0176-1617(96)80081-2
- Linderholm HW (2006) Growing season changes in the last century.

 Agric For Meteorol 137:1–14. https://doi.org/10.1016/j.agrformet.2006.03.006
- McKown AD, Guy RD, Azam MS, Drewes EC, Quamme LK (2013) Seasonality and phenology alter functional leaf traits. Oecologia 172:653–665. https://doi.org/10.1007/s00442-012-2531-5
- Merzlyak MN, Gitelson AA, Chivkunova OB, Rakitin VY (1999) Non-destructive optical detection of pigment changes during leaf senescence and fruit ripening. Physiol Plant 106:135–141. https://doi.org/10.1034/j.1399-3054.1999.106119.x

- Morgan PW (1984) Is ethylene the natural regulator of abscission? In: Fuchs Y, Chalutz E (eds) Ethylene: biochemical, physiological and applies aspects. Martinus Nijhoff, The Hague, pp 231–240
- Mostowska A (2005) Leaf senescence and photosynthesis. In: Pessarakli M (ed) Handbook of Photosynthesis. CRC Press, Taylor and Francis Group, Boca Raton, Florida, pp 691–716
- National Centers for Environmental Information, Data tools: 1981–2010 normals. http://www.ncdc.noaa.gov/cdo-web/datatools/normals. Accessed 31 Mar 2016
- Neilsen D, Millard P, Neilsen GH, Hogue EJ (1997) Sources of N for leaf growth in a high-density apple (*Malus domestica*) orchard irrigated with ammonium nitrate solution. Tree Physiol 17:733–739
- Noda HM, Muraoka H, Nasahara KN, Saigusa N, Murayama S, Koizumi H (2015) Phenology of leaf morphological, photosynthetic, and nitrogen use characteristics of canopy trees in a cool-temperate deciduous broadleaf forest at Takayama, central Japan. Ecol Res 30:247–266. https://doi.org/10.1007/s11284-014-1222-6
- Onoda Y, Hikosaka K, Hirose T (2004) Allocation of nitrogen to cell walls decreases photosynthetic nitrogen-use efficiency. Funct Ecol 18:419–425
- Parmesan C, Yohe G (2003) A globally coherent fingerprint of climate change impacts across natural systems. Nature 421:37–42. https://doi.org/10.1038/nature01286
- Peguero-Pina JJ, Morales F, Flexas J, Gil-Pelegrin Moya I (2008)
 Photochemistry, remotely sensed physiological reflectance index and de-epoxidation state of the xanthophyll cycle in *Quercus coccifera* under intense drought. Oecologia 156:1–11. https://doi.org/10.1007/s00442-007-0957-y
- Penuelas J, Frederic B, Filella I (1995) Semi-empirical indices to assess carotenoids/chlorophyll-a ratio from leaf spectral reflectance. Photosynthetica 31:221–230
- Plummer M (2003) JAGS: A program for analysis of Bayesian graphical models using Gibbs sampling. Working Papers 8
- Plummer M (2018) rjags: Bayesian Graphical Models using MCMC. R package version 4-8. https://CRAN.R-project.org/package=rjags. Accessed 1 July 2018
- R Core Team (2017) R: A language and environment for statistical computing. R Foundation for Statistical Computing, Vienna, Austria. https://www.R-project.org/. Accessed 1 July 2018
- Richardson AD, Anderson RS, Arain MA, Barr AG, Bohrer G, Chen G, Chen JM, Ciais P, Davis KJ, Desai AR, Dietze MC, Dragoni D, Garrity SR, Gough CM, Grant R, Hollinger DY, Margolis HA, McCaughey H, Migliavacca M, Monson RK, Munger JW, Poulter B, Raczka BM, Ricciuto DM, Sahoo AK, Schaefer K, Tian H, Vargas R, Verbeeck H, Xiao J, Xue Y (2012) Terrestrial biosphere models need better representation of vegetation phenology: results from the North American Carbon Program Site Synthesis. Glob Change Biol 18:566–584. https://doi.org/10.1111/j.1365-2486.2011.02562.x
- Richardson AD, Hufkens K, Milliman T, Aubrecht DM, Furze ME, Seyednasrollah B, Krassovski MB, Latimer JM, Nettles WR, Heiderman RR, Warren JM, Hanson PJ (2018) Ecosystem warming extends vegetation activity but heightens vulnerability to cold temperatures. Nature 560:368–371. https://doi.org/10.1038/s41586-018-0399-1
- Sage RF, Pearcy RW, Seemann JR (1987) The nitrogen use efficiency of C3 and C4 plants: III. Leaf nitrogen effects on the activity of carboxylating enzymes in *Chenopodium album* (L.) and *Amaranthus retroflexus* (L). Plant Physiol 85:355–359. https://doi.org/10.1104/pp.85.2.355
- Serbin SP, Singh A, McNeil BE, Kingdon CC, Townsend PA (2014) Spectroscopic determination of leaf morphological and biochemical traits for northern temperate and boreal tree species. Ecol Appl 24:1651–1669



- Sims DA, Gamon JA (2002) Relationships between leaf pigment content and spectral reflectance across a wide range of species, leaf structures and developmental stages. Remote Sens Environ 81:337–354. https://doi.org/10.1016/S0034-4257(02)00010-X
- Stylinksi CD, Gamon JA, Oechel WC (2002) Seasonal patterns of reflectance indices, carotenoid pigments and photosynthesis of evergreen chaparral species. Oecologia 131:366–374. https://doi.org/10.1007/s00442-002-0905-9
- Taiz K, Zeiger E (2006) Plant Physiology, 4th edn. Massachussetts, Sinauer Associates Inc, Sunderland, p 411/583
- Van Gaalen KE, Flanagan LB, Peddle DR (2007) Photosynthesis, chlorophyll fluorescence and spectral reflectance in *Sphagnum* moss at varying water contents. Oecologia 153:19–28. https://doi. org/10.1007/s00442-007-0718-y
- Vargas R (2012) How a hurricane disturbance influences extreme CO₂ fluxes and variance in a tropical forest. Environ Res Lett 7:035704. https://doi.org/10.1088/1748-9326/7/3/035704
- Vogelmann JE, Rock BN, Moss DM (1993) Red edge spectral measurements from sugar maple leaves. Int J Remote Sens 14:1563–1575. https://doi.org/10.1080/01431169308953986
- USDA NRCS Soil Survey, WebSoilSurvey. http://websoilsurvey. sc.egov.usda.gov/App/WebSoilSurvey.aspx. Accessed 31 Mar 2003

- Wheeler KI, Levia DF, Hudson JE (2017) Tracking senescence-induced patterns in leaf litter leachate using parallel factor analysis (PARAFAC) modeling and self-organizing maps. J Geophys Res Biogeo 122:2233–2250. https://doi.org/10.1002/2016JG003677
- Xue L, Cao W, Luo W, Dai T, Zhu Y (2004) Monitoring leaf nitrogen status in rice with canopy spectral reflectance. Agron J 96:135–142. https://doi.org/10.2134/agronj2004.1350
- Yang X, Tang J, Mustard JF, Wu J, Zhao K, Serbin S, Lee J-E (2016) Seasonal variability of multiple leaf traits captured by leaf spectroscopy at two temperate deciduous forests. Remote Sens Environ 179:1–12. https://doi.org/10.1016/j.rse.2016.03.026
- Zhang X, Friedl MA, Schaaf CB, Strahler AH, Hodges JCF, Gao F, Reed BC, Huete A (2003) Monitoring vegetation phenology using MODIS. Remote Sens Environ 84:471–475. https://doi.org/10.1016/S0034-4257(02)00135-9
- Zhu Y, Yao X, Tian Y, Liu X, Cao W (2008) Analysis of common canopy vegetation indices for indicating leaf nitrogen accumulations in wheat and rice. Int J Appl Earth Obs Geoinf 10:1–10

Affiliations

Kathryn I. Wheeler^{1,2} • Delphis F. Levia^{1,3} • Rodrigo Vargas^{1,3}

- Department of Geography and Spatial Sciences, University of Delaware, Newark, DE, USA
- Department of Earth and Environment, Boston University, Boston, MA, USA
- Department of Plant and Soil Sciences, University of Delaware, Newark, DE, USA

